Nanoorganization of Reactive Mixtures of Mid-Functional Polystyrene with End-Functional Oligomer

Isamu Akiba,* Kanako Nomura, Kyoko Shikasho, Yeonhwan Jeong, and Kazuo Sakurai

Department of Chemical Environments and Processes, Faculty of Environmental Engineering, The University of Kitakyushu, 1-1 Hibikino, Wakamatsu, Kitakyushu, Fukuoka 808-0135, Japan

Received June 12, 2003
Revised Manuscript Received September 10, 2003

Introduction

Blends and composites of two different polymers are versatile ways to develop novel polymeric materials. In these systems, nanostructures have lately attracted attention because of its characteristic properties.[1−4] Therefore, the establishment of the method to control nanostructures in these systems is of importance.

In polymer−polymer or polymer−oligomer mixtures, it is widely accepted that attractive interactions and reactions between components strongly affect miscibility and aggregated structure.[1,5−11] Hence, it is expected that they are effective in controlling nanoorganized structures in the blends. However, if the associations and reactions between the components randomly occur along the polymer chains, the blends form randomly aggregated structures or merely miscible mixtures.[6−11] To construct nanoorganized structures, architecture of the component molecules is required.[1,9,12,13] When the component polymers are joined to each other at specific positions in the polymer chains, the blends should form the organized structures reflecting the molecular structures.[1,2,12−21] The present paper reports on the self-organization of the reactive mixtures of polystyrene having a pyridyl group at the chain center with 1-bromoeicosane or 1-bromooctadecane as model compounds of end-functional oligomers.

Experimental Section

Materials. Styrene (**1**) was purchased from Wako Pure Chemicals Co., Ltd. *sec*-Butyllithium (*sec*-BuLi) in 1 mol L^{-1} hexane solution was purchased from Kanto Chemicals Co., Ltd. 1,1-Diphenylethylene (**2**), 2,6-bisbromomethylpyridine (**3**), 1-eicosyl bromide (EICO), and 1-octadecyl bromide (OCTD) were purchased from Tokyo Chemical Industry Co., Ltd. The **1** and **2** were purified with activated alumina.

Synthesis of Mid-Functional Polystyrene. Polystyrene having a pyridyl group at the chain center (DPP) was synthesized following Scheme 1 with conventional living anionic polymerization technique. **1** was polymerized using *sec*-BuLi as initiator. The resulting living polystyryllithium was end-capped with **2**. A part of the solution was taken out to obtain reference polystyrene (PS). Subsequently, the living anions were deactivated by **3** in sufficiently cooled conditions. Residual living anions were deactivated with methanol. The resulting solution was reprecipitated in methanol. The resulting material was fractionated by fractional precipitation. The final DPP and the reference PS were characterized by gel permeation chromatography (GPC) and elemental analysis. The results of the characterizations of PS and DPP are shown in Figure 1 and Table 1. The molecular weight of DPP was about twice larger than that of PS, and the polydispersity was unchanged by the coupling reaction. The pyridine content of DPP was equivalent to about 1 pyridine unit per 38 styrene units. This value corresponds to 1 pyridine unit in one chain of DPP.

* To whom correspondence should be addressed: e-mail akiba@env.kitakyu-u.ac.jp.

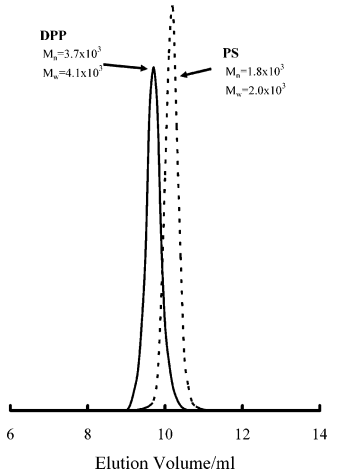

Figure 1. GPC elugrams of PS and DPP. Estimated molecular weight of DPP is twice that of PS.

Table 1. Molecular Characteristics of PS and DPP

samples	$M_w \times 10^3$ [a]	$M_n \times 10^3$ [a]	M_w/M_n	pyridine content[b] (mol %)
PS	2.0	1.8	1.1	0
DPP	4.1	3.8	1.1	2.6[c]

[a] Obtained from GPC. [b] Pyridine content is calculated from the elemental analysis data of carbon, hydrogen, and nitrogen. [c] The pyridine content is equivalent to about 1 pyridine unit per 38 styrene units. This value indicates that DPP contains one pyridine unit in one chain.

Preparation of DPP−EICO and DPP−OCTD Mixtures. DPP and EICO were weighted to the desired composition and dissolved in toluene/DMF 1/1 (v/v). The amounts of pyridyl group of DPP to EICO in the mixtures are set in the molar ratio of 1.0 to 1.2 (DPP−EICO1) and 2.0 to 1.0 (DPP−EICO2). The solutions were stirred at 60 °C for 72 h, and then reaction shown in Scheme 2 occurred. After this procedure, the solutions were poured into a large amount of methanol. The resulting mixtures were washed by hexane to remove residual EICO. In a similar manner as above, the DPP−OCTD mixture in which the ratio of pyridyl group of DPP to OCTD is set in the molar ratio of 1.0 to 1.2 was prepared. The mixtures were dried in reduced pressure for 1 week. Final ratios of pyridyl group of DPP to EICO or OCTD determined by elemental analyses were in molar ratios of 1.0 to 1.05 for DPP−EICO1, 2.0 to 1.0 for DPP−EICO2, and 1.0 to 1.0 for DPP−OCTD.

Differential Scanning Calorimetry (DSC). DSC measurements were carried out using a Perkin-Elmer Pyris 1 DSC. All the DSC measurements were performed under N_2 flow and at a heating rate of 10 °C/min. Data in the second scanning were employed.

Small-Angle X-ray Scattering (SAXS). SAXS measurements were carried out at the BL40B2 station at SPring-8 in Japan. The SAXS measurements were performed at ambient temperature for the samples annealed at 60 °C to remove any internal strains. Two-dimensional SAXS patterns were obtained by a Rigaku R-AXIS IV++ imaging plate. The one-dimensional SAXS profiles ($I(q)$ vs q, where I and q denote the scattering intensity and the magnitude of the scattering vector) were converted from the two-dimensional SAXS patterns by circular averaging.

10.1021/ma0348019 CCC: $25.00
Published on Web 10/23/2003

Scheme 1. Synthetic Pathway to the Polystyrene Having a Pyridine Unit at Chain Center

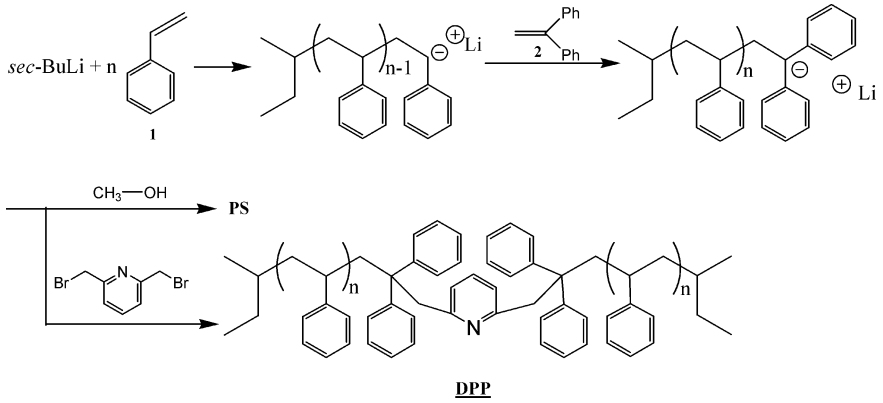

Scheme 2. Reaction between DPP and EICO during the Mixing Procedure

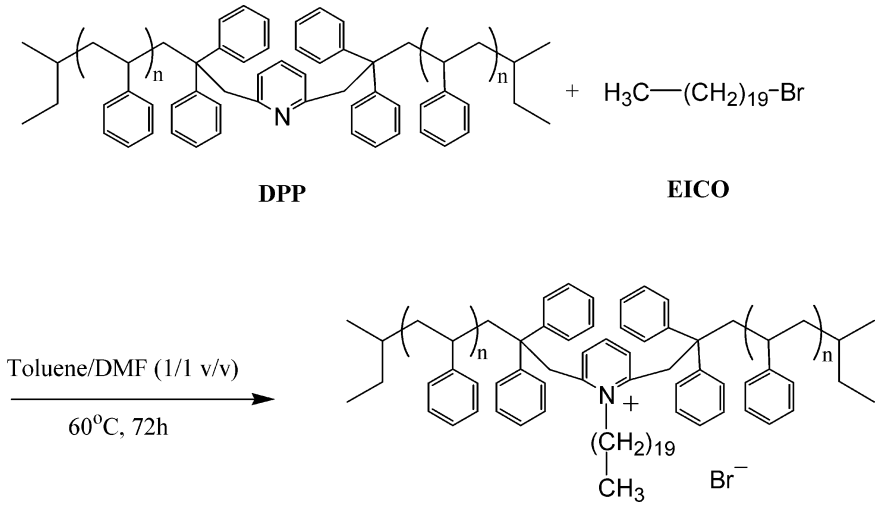

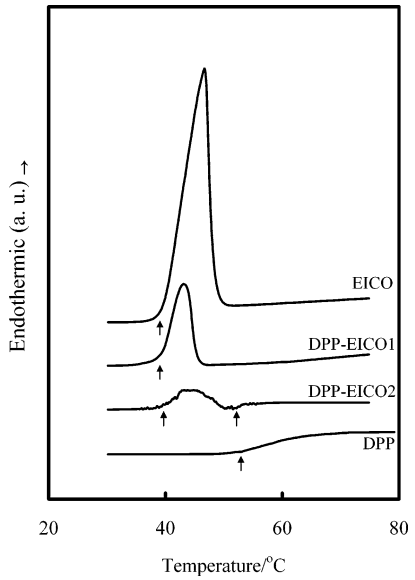

Figure 2. DSC thermograms of DPP, EICO, DPP−EICO1, and DPP−EICO2. The arrows in this figure indicate the onset point of melting and glass transitions.

Results and Discussion

Figure 2 shows DSC thermograms for DPP, EICO, DPP−EICO1, and DPP−EICO2. EICO and DPP−EICO1 show endothermic peaks around 40 °C. The peaks are attributed to melting of crystalline packing of eicosyl chains. The onset point of the melting peak, i.e., melting temperature (T_m), of DPP−EICO1 is at 40 °C, which is almost same as that of EICO. DPP−EICO2 also shows a melting peak around 40 °C. In addition, DPP−EICO2 shows a glass transition in a similar manner as DPP. The glass transition temperatures (T_g) of both DPP−EICO2 and DPP are estimated at 53 °C. If the mixtures of DPP and EICO are miscible, it should be expected that T_g and T_m of the mixtures are drastically depressed from the T_g of DPP and the T_m of EICO, respectively. Therefore, it is considered that DPP and EICO are phase-separated in the mixtures. However, macroscopic phase separations in DPP−EICO mixtures are not observed in both the molten and solid state. Hence, it is expected that the phase separation of the DPP−EICO mixtures occurs in nanospaces. Then, the SAXS measurements for the DPP−EICO mixtures are performed. In addition to the effect of alkyl chain length on the phase structures, the SAXS measurements are also performed for DPP−OCTD.

Figure 3 shows the SAXS profiles of EICO, DPP−EICO1, and DPP−EICO2. Although the data are not shown here, we have confirmed that SAXS from DPP does not show any peaks. The SAXS profile of EICO shows diffraction peaks up to third-order diffraction at the q positions relatively assigned to 1:2:3. Therefore, EICO forms well-ordered crystalline lamellar structure. The periodic length of the lamellar structure of EICO estimated from the first-order diffraction is 5.0 nm, which closely corresponds to twice the length of the eicosyl group with a planar zigzag conformation. Therefore, EICO forms an end-to-end double-layer structure. On the other hand, the SAXS profile of DPP−EICO1

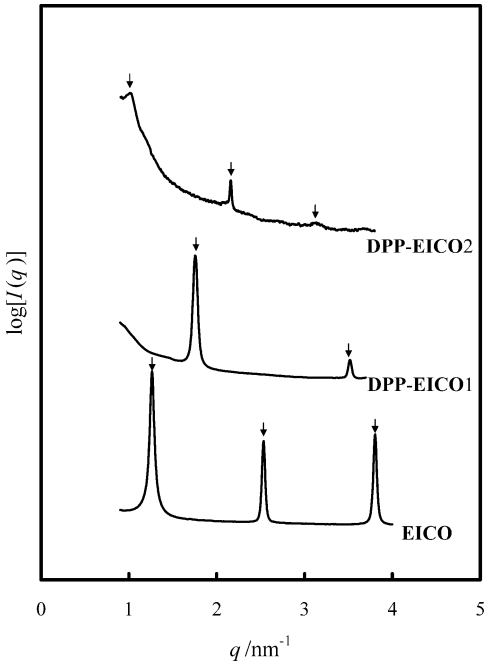

Figure 3. SAXS profiles of EICO, DPP−EICO1, and DPP−EICO2. The arrows indicate the positions of scattering peaks.

clearly shows diffraction peaks up to second-order diffraction at the q positions relatively assigned to 1:2. Therefore, DPP−EICO1 also forms a lamellar structure. However, its periodic length estimated from first-order diffraction is 3.6 nm, which is shorter than that of EICO. Similarly, since the SAXS profiles of DPP−EICO2 show diffraction peaks up to third-order diffraction at the q position relatively assigned to 1:2:3, it also forms the lamellar structure. In contrast to DPP−EICO1, the periodic length of the lamellar of DPP−EICO2 is estimated to 6.0 nm, which is longer than that of EICO. Hence, the periodic length of the lamellar structure of DPP−EICO mixtures strongly depends on the composition of the mixtures. It is expected that the ordered structures of the DPP−EICO mixtures also depend on the alkyl chain length. Figure 4 shows SAXS profiles of the DPP−EICO1 and DPP−OCTD mixtures. DPP−OCTD shows diffraction peaks up to second-order diffraction. Since the q positions of the diffraction peaks are relatively assigned to 1:2, DPP−OCTD also forms the lamellar structure. The periodic length of the lamellar of DPP−OCTD is 3.4 nm, which is slightly shorter than that of DPP−EICO1. The difference between the periodic lengths of DPP−EICO1 and DPP−OCTD closely corresponds to the difference between chain lengths of EICO and OCTD with the planar zigzag conformation (∼0.15 nm). Therefore, it is considered that the alkyl chains in these systems are vertically oriented to the lamellar plane.

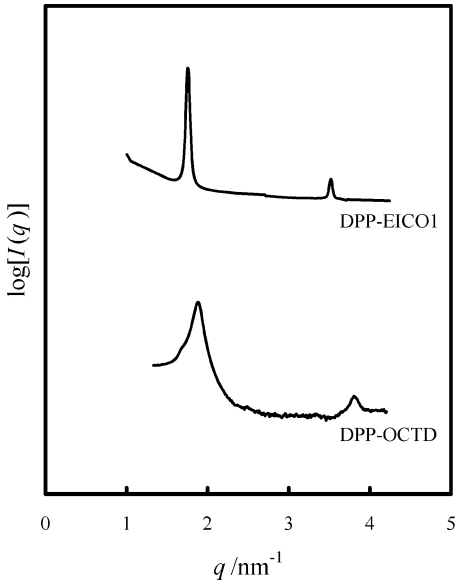

Figure 4. SAXS profiles of DPP−EICO1 and DPP−OCTD.

On the basis of the SAXS results, the mesomorphically organized structures of the DPP−EICO mixtures are schematically represented as Figure 5. Since chain length of EICO taking the optimum (planar zigzag) conformation is estimated at 2.5 nm by MOPAC calculations, the lamellar structure of EICO, which has a 5.0 nm periodic length, takes an end-to-end double-layer structure as shown in Figure 5a. On the other hand, the periodic length of DPP−EICO1 is shorter than that of EICO but longer than the chain length of EICO taking the optimum conformation. In addition, the alkyl

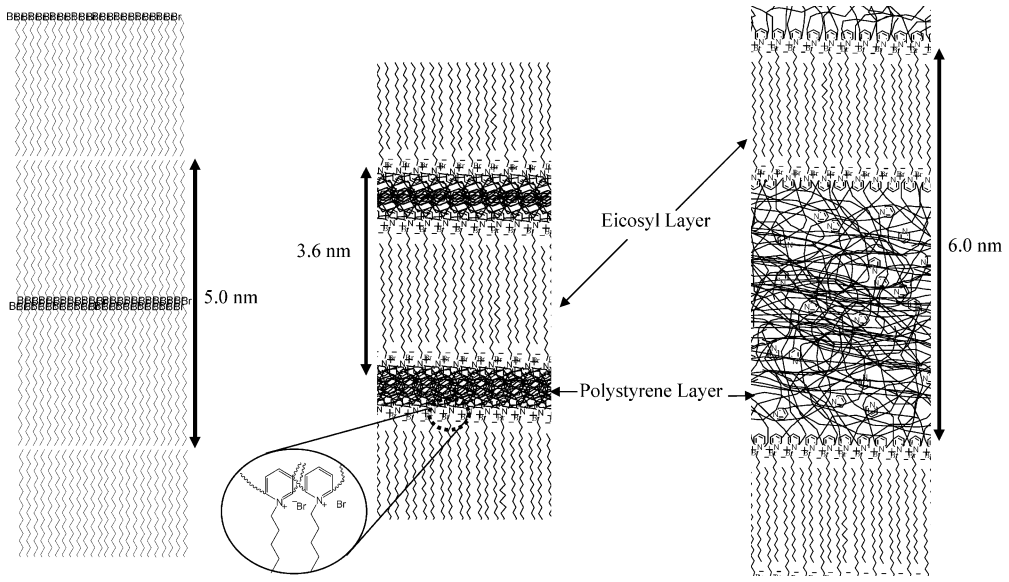

Figure 5. Schematic representation of the organized structure of EICO, DPP−EICO1, and DPP−EICO2.

chains are vertically oriented to the lamellar plane as mentioned above. Therefore, it is considered that the eicosyl chains in DPP−EICO1 form interdigitating packing between the DPP layers as shown in Figure 5b. However, it seems difficult to take the ordered structure shown in Figure 5b in whole space because of restrictions of molecular structure, such as steric hindrance, of DPP. In addition, the volume ratio of EICO to DPP (ca. 1:4) in DPP−EICO1 is not consistent with the lamellar structure. On the other hand, it is reasonable that the alkyl chains are vertically oriented to the lamellar interface because of the dependence of the periodic length of the lamellar structure on the alkyl chain length. Therefore, it is considered that DPP−EICO1 contains a large amount of amorphous region, or there are many defects in the lamellar structure of DPP−EICO1 to get rid any stresses around the interface and on the volume fraction. In fact, there are many eicosyl chains which do not join in the crystalline packing because the heat of fusion of EICO in DPP−EICO1 (27 kJ (mol of EICO)$^{-1}$ estimated by DSC) is much smaller than that of EICO alone (48 kJ mol^{-1}). In the DPP−EICO2, periodic length of the lamellar becomes longer than that of EICO. In DPP−EICO2, there are large amounts of residual DPP against EICO. Since DPP strongly segregates against EICO, the residual DPP must dissolve in the DPP layer. Hence, as shown in Figure 5c, the thickness of the DPP layer is enlarged due to the residual DPP, and consequently the periodic length of the lamellar of the DPP−EICO2 becomes longer.

Acknowledgment. SAXS measurements were performed at the SPring-8 with the approved number 2002A0604-NL2-np. Elemental analyses and DSC measurements were performed at The Instrumentation Center of The University of Kitakyushu. A part of this work is supported by funding from the Japanese Ministry of ECSST via the Kitakyushu Knowledge-based Cluster Project.

References and Notes

(1) Kato, T. *Struct. Bonding (Berlin)* **2000**, *96*, 95.
(2) Kato, T. *Kobunshi* **2003**, *52*, 276.
(3) Hamley, I. W. *Angew. Chem., Int. Ed.* **2003**, *42*, 1692.
(4) Kato, M.; Usuki, A. *Seikeikakou* **2002**, *14*, 222.
(5) Coleman, M. M.; Graf, J. F.; Painter, P. C. *Specific Interaction and the Miscibility of Polymer Blends*; Technomic: Lancaster, 1991.
(6) Lee, J. Y.; Painter, P. C.; Coleman, M. M. *Macromolecules* **1988**, *21*, 954.
(7) Lange, R. F. M.; Meijer, E. W. *Macromolecules* **1995**, *28*, 782.
(8) Avramova, N. *Polymer* **1995**, *36*, 801.
(9) Hobbie, E. K.; Han, C. C. *J. Chem. Phys.* **1996**, *195*, 738.
(10) Akiba, I.; Ohba, Y.; Akiyama, S. *Macromolecules* **1999**, *32*, 1175.
(11) Charoensirisomboon, P.; Chiba, T.; Solomko, S. I.; Inoue, T.; Weber, M. *Polymer* **1999**, *40*, 6830.
(12) Sato, A.; Kato, T.; Uryu, T. *J. Polym. Sci., Polym. Chem. Ed.* **1996**, *34*, 503.
(13) Tanaka, F.; Ishida, M.; Matsuyama, A. *Macromolecules* **1991**, *24*, 5582.
(14) Akiba, I.; Akiyama, S. *Macromolecules* **1999**, *32*, 3741.
(15) Akiba, I.; Akiyama, S. *Mol. Cryst. Liq. Cryst.* **2000**, *339*, 209.
(16) Akiba, I.; Sakurai, K. *e-Polym.* **2002**, 053.
(17) Ruokolainen, J.; ten Brinke, G.; Ikkala, O.; Torkkeli, M.; Serimaa, R. *Macromolecules* **1996**, *29*, 3409.
(18) Luyten, M. C.; Alberda van Ekenstein, G. O. R.; ten Brinke, G.; Ruokolainen, J.; Ikkala, O.; Torkkeli, M.; Serimaa, R. *Macromolecules* **1999**, *32*, 4404.
(19) Iwasaki, K.; Hirao, A.; Nakahama, S. *Macromolecules* **1993**, *26*, 2626.
(20) Haraguchi, M.; Nakagawa, T.; Nose, T. *Polymer* **1995**, *36*, 2567.
(21) Inomata, K.; Liu, L.-Z.; Nose, T.; Chu, B. *Macromolecules* **1999**, *32*, 1554.

MA0348019